Liquid Crystals

Publication details, including instructions for authors and subscription information:
http://www.informaworld.com/smpp/title~content=t713926090

Liquid crystal birefringence for millimeter wave radar

K. C. Lim[a]; J. D. Margerum[a]; A. M. Lackner[a]; L. J. Miller[a]; E. Sherman[a]; W. H. Smith Jr.[a]
[a] Hughes Research Laboratories, Malibu, California, USA

To cite this Article Lim, K. C. , Margerum, J. D. , Lackner, A. M. , Miller, L. J. , Sherman, E. and Smith Jr., W. H.(1993) 'Liquid crystal birefringence for millimeter wave radar', Liquid Crystals, 14: 2, 327 — 337

To link to this Article: DOI: 10.1080/02678299308027647

URL: http://dx.doi.org/10.1080/02678299308027647

LIQUID CRYSTALS, 1993, VOL. 14, NO. 2, 327–337

Liquid crystal birefringence for millimeter wave radar

by K. C. LIM, J. D. MARGERUM*, A. M. LACKNER, L. J. MILLER,
E. SHERMAN and W. H. SMITH, JR.

Hughes Research Laboratories, 3011 Malibu Canyon Road,
Malibu, California 90265, USA

Many liquid crystals are found to have relatively high birefringence (Δn) values in the microwave and millimeter wave regions, as calculated from the phase shift induced by their reorientation by magnetic or electric fields. At 30 GHz, Δn values were obtained in the range of 0·08 to 0·18 for eleven liquid crystal mixtures of various types. The most favourable liquid crystal structures for high millimeter wave birefringence are highly conjugated rod-like molecules containing biphenyl, terphenyl, phenylpyrimidine, biphenylpyrimidine, and tolane groups in nematics of positive dielectric anisotropy ($\Delta\varepsilon$). However, other liquid crystal structures including Schiffs base, azoxybenzene, and aromatic ester groups also have substantial birefringence, including nematics with negative and crossover $\Delta\varepsilon$, as well as cholesteric nematics. The Δn varied only slightly at different frequencies of microwave millimeter wave in the 15–94 GHz range. Studies on magnetic and electrical field liquid crystal orientation in specially designed waveguides provide a basis for new types of modulators and scanning array antennae in the millimeter wave region, where more compact liquid crystal modulation media can be used than in the microwave region. These scanners can be used for both sending and receiving radar signals for potentially low cost radar systems.

1. Introduction

We found that many thermotropic liquid crystals have a surprisingly high birefringence (Δn) in the microwave and millimeter wave regions. The visible light birefringence of liquid crystals is well known to be associated with their anisotropic molecular polarizabilities and is related to their electronic band transitions in the ultraviolet region (above about 10^{15} Hz) [1, 2]. It has also been shown that this birefringence extends well into the infrared region (in the 10^{13} Hz range), where it is also affected by anisotropy of vibrational molecular motions [3, 4]. However, as indicated in figure 1, the microwave region (1–30×10^9 Hz) and the millimeter wave region (30–100×10^9 Hz) [5] have much lower frequencies and much longer wavelengths than the visible and infrared regions. At somewhat lower frequencies in the MHz region (10^6–10^9 Hz), it is well known that Debye type molecular relaxation processes often cause changes in organic molecules [6] and in the magnitude and sign of the liquid crystal dielectric anisotropy ($\Delta\varepsilon$) properties. Thus, we had not expected to find substantial Δn values for liquid crystals through a wide range of the microwave–millimeter wave region.

In this work, we report for the first time phase shifts in the millimeter wave region induced by field reorientation of liquid crystals in waveguides. These phase shifts are used to calculate the millimeter wave Δn values of several different types of

---

*Author for correspondence.

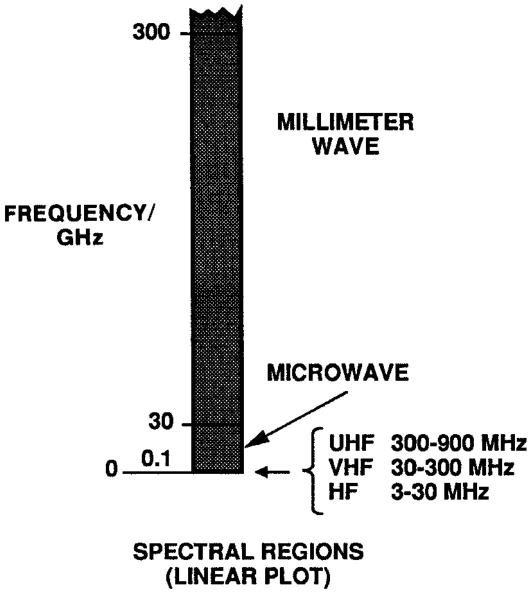

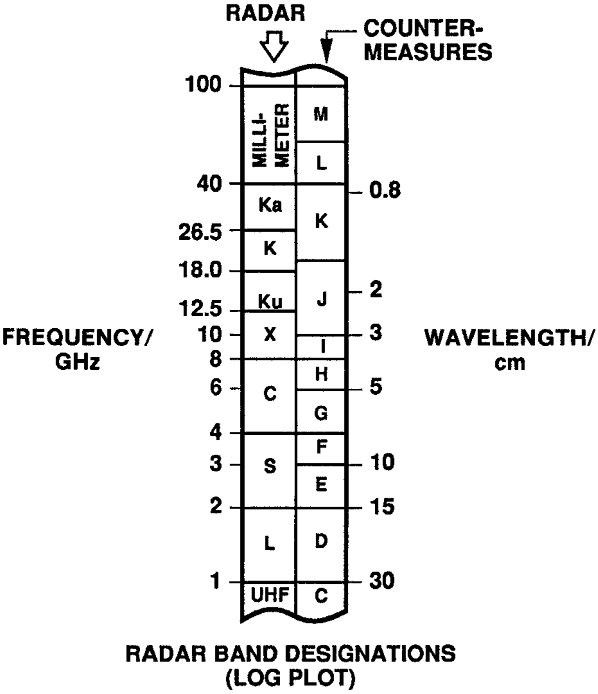

Figure 1. Diagram of electromagnetic spectrum and radar band designations.

thermotropic liquid crystals, from which some preliminary correlations are made between liquid crystal structures and their millimeter wave birefringence. These results are the basis for the development of potentially low cost modulators, and scanning phased array antennae for radar system applications.

2. Experimental

The millimeter wave refractive indices of liquid crystals were measured at 30 GHz and 94 GHz with a waveguide version of a Mach–Zehnder interferometer [7], and in the 15–75 GHz region with a vector network analyser, using external magnets to orient the bulk liquid crystals. The liquid crystal birefringence values were measured mainly with a 30 GHz TE_{10} mode rectangular waveguide version of the Mach–Zehnder interferometer (or phase bridge), using the simplifying approximation that the Δn was directly related to the phase shift difference ($\Delta\theta$) caused by changing the transverse H-field orientation from perpendicular to parallel to the millimeter wave E-vector in the waveguide, as indicated in equation (1), where λ_0 is the free space millimeter wave wavelength and d is the path length of liquid crystal reoriented along the waveguide axis

$$\Delta n = n_e - n_o = \Delta\theta\lambda_0/2\pi d. \tag{1}$$

The liquid crystal sample was contained inside a section of the waveguide in one arm of the phase bridge, and the phase shifts caused by the liquid crystal and its reorientation were compensated by a calibrated phase shifter in the other arm, as indicated in figure 2. Two 5 kG permanent magnets, with large cross section areas, were mounted externally to apply a fairly uniform H-field through the whole length of the waveguide section containing the liquid crystal. For Δn measurements, the magnets were mounted such that the magnetic field was aligned either parallel or transversely perpendicular to the E-field vector of the propagating millimeter wave inside the waveguide sample cell.

A rectangular millimeter waveguide cross-section is shown in figure 3, showing the propagation direction of the millimeter wave and an arbitrary angle ϕ between the millimeter wave E-vector and the orientation of the liquid crystal director. The inside dimensions of the 30 GHz waveguides were 7·11 × 3·56 mm.

Phase shifts induced by electrical field (E-field) reorientation of liquid crystals were also studied, using a special cell, shown in figure 4, which had electrodes in opposite walls of the waveguide. Phase shift differences were studied between the voltage induced E-field orientation of liquid crystals parallel to the millimeter wave E-vector and H-field orientation of liquid crystals perpendicular to the E-vector.

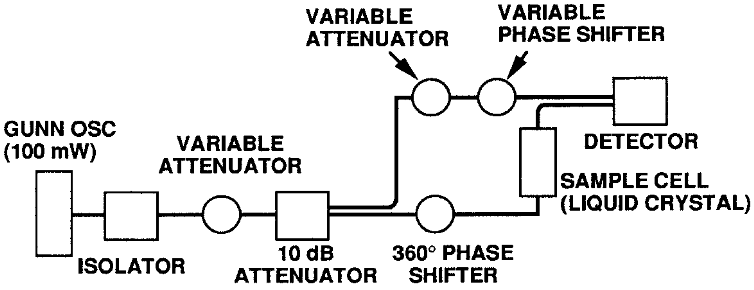

Figure 2. Diagram of a phase bridge apparatus for liquid crystal studies: a 30 GHz TE_{10} mode waveguide Mach–Zehnder interferometer.

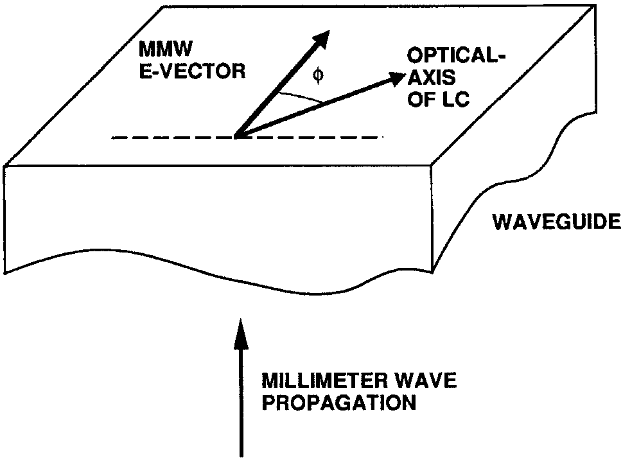

Figure 3. Diagram of orientation angle ϕ between the liquid crystal director and the E-vector of the millimeter wave in a waveguide.

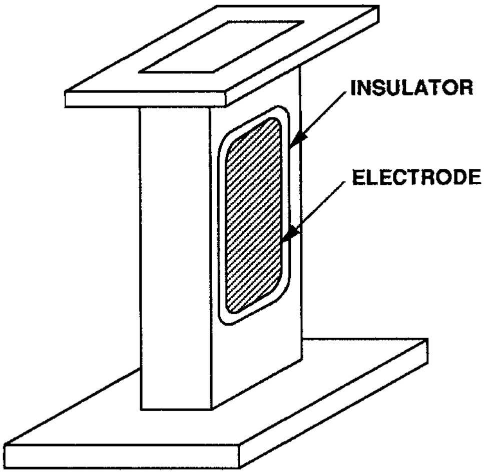

30 GHz WAVEGUIDE SECTION

Figure 4. Diagram of a 30 GHz waveguide cell with electrodes for liquid crystal orientation.

3. Results and discussion

3.1. *H-Field orientation of liquid crystals*

In one set of experiments, the angle ϕ between the H-field liquid crystal orientation direction and the millimeter wave E-vector (see figure 3) was varied continuously between $-90°$ and $+90°$. The resulting room temperature phase shifts ($\Delta\theta$) caused by these changes in liquid crystal orientation are shown in figure 5 for three different liquid crystals, using a 2·5 cm path length in the 30 GHz waveguide. The phase shift varied continuously with the orientation direction, with the largest $\Delta\theta$ at 0° where the liquid crystal director was parallel to the millimeter wave E-vector. As the liquid crystals were reoriented through 90° the phase shift showed a region of fairly linear response. This is an important characteristic for many device applications. Figure 5 shows that the millimeter wave Δn of ROTN-404 and BDH-E7 are considerably higher than that of BDH-K15 at room temperature. The approximate Δn values were calculated to be 0·17, 0·16, and 0·10, respectively, for these liquid crystals.

The phase shift was also found to be linearly dependent upon the path length of the liquid crystal that was reoriented in the waveguide. This effect is shown in figure 6 for orthogonal H-field reorientation of BDH-BL006 in the range of 0–2 cm path length at 30 GHz. Its birefringence was calculated to be 0·18.

Table 1 shows a summary of the millimeter wave birefringence of liquid crystal mixtures studied by phase shifts from H-field reorientation at 30 GHz. This table also

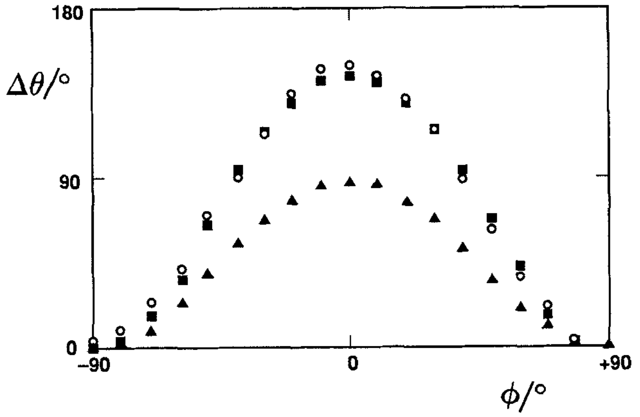

Figure 5. Effect on the relative phase shift at 30 GHz of the orientation angle ϕ between millimeter wave E-vector and the liquid crystal director as aligned by an external magnetic field on a 2·5 cm path length of three different liquid crystals: (○) ROTN-404, (■) BDH-E7, and (▲) BDH-K15.

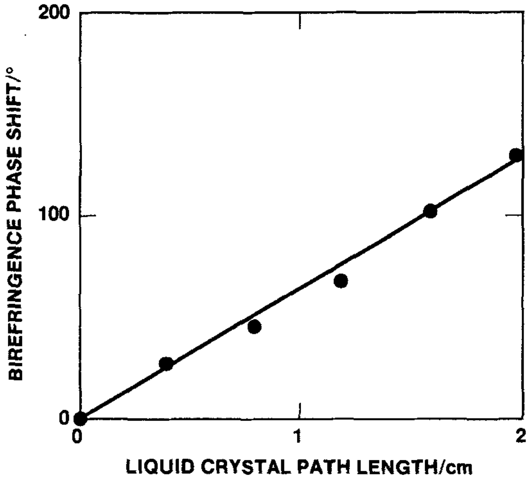

Figure 6. Effect of the liquid crystal path length on the phase shift when the magnetic field alignment of BDH-BL006 was switched from perpendicular to parallel to the E-vector of the 30 GHz millimeter wave; $\Delta n = 0{\cdot}18$.

Table 1. Calculated millimeter wave birefringence at 30 GHz of various types of liquid crystal mixtures, and a comparison with their visible birefringence. (From phase shifts with orthogonal H-field orientation of the liquid crystals, which did not fully align BDH-16963 to its nematic phase).

Liquid crystal	Liquid crystal structure types	$\Delta\varepsilon$	Millimeter wave Δn (30 GHz)	Visible Δn (589 nm)	Ratio Δn Millimeter wave/visible
BDH-BL007	(Cyanobiphenyls?)	+14·1	0·180	0·287	63%
ROTN-404	Cyanobiphenyls, cyanophenylpyrimidines	+21·4	0·166	0·268	62%
Tolane I/II	Alkyl–alkoxytolanes	+0·2	0·163	0·226	72%
BDH-E7	Cyanobiphenyls, cyanoterphenyls	+11	0·160	0·225	71%
Merck-NP5	Azoxybenzene	−0·2	0·147	0·290	51%
ZLI-1085	Esters, diesters (crossover)	+0·8, −0·9	0·114	0·170	67%
MBBA	Schiffs-base	−0·5	0·106	0·227	47%
BDH-K15	Cyanobiphenyl	+11	0·098	0·184	53%
BDH-16963	Chiral nematic (cholesteric nematic phase transition)	—	(0·091)	0·198	46%
HRL-NP55	Esters (cyanophenyl benzoates)	+17·1	0·082	0·150	55%

Table 2. Phase shifts and birefringence values for two liquid crystals (BDH-E7 and ROTN-404) over the 15–94 GHz range, using a network analyser for the 15–75 GHz range and a phase bridge for the 94 GHz measurement. (Phase shifts from orthogonal magnetic field orientation of the liquid crystals.)

Microwave Frequency GHz	Microwave Wavelength cm	BDH-E7		ROTN-404	
		$\Delta\theta$/cm	Approx. Δn	$\Delta\theta$/cm	Approx. Δn
15	2·0	19	0·11	—	—
30	1·0	40	0·11	51	0·14
60	0·5	100	0·14	120	0·17
75	0·4	120	0·13	155	0·17
94	0·32	182	0·16		

gives a description of the general structural types of their components, their values of dielectric anisotropy (measured at 1 kHz), their visible Δn values at 589 nm, and the ratio of their Δn_{MMW} divided by Δn_{vis}. In table 1 the liquid crystals are listed in the order of their measured millimeter wave Δn values, with the highest at the top. The magnetic field was assumed to give good bulk alignment of the liquid crystals, although it was not strong enough fully to align the chiral nematic sample (BDH-16963) to the nematic phase such as is obtained with applied electric fields. The most favourable liquid crystal structures for high millimeter wave Δn are highly conjugated rod-like molecules containing biphenyl, terphenyl, phenylpyrimidine, biphenylpyrimidine, and tolane groups. The millimeter wave Δn values were in the range 62–72 per cent of the visible Δn values for these positive $\Delta\varepsilon$ nematic liquid crystals. However, other liquid crystal structures including Schiffs base, azoxybenzene, and aromatic ester groups also showed substantial birefringence, including nematics with negative $\Delta\varepsilon$ (Merck-NP5 and MBBA) and crossover $\Delta\varepsilon$ (ZLI-1085), as well as a chiral nematic (BDH-16963). These other structures showed millimeter wave Δn values in the range of 46–67 per cent of the visible Δn values. The fact that the millimeter wave Δn of the crossover liquid crystal was 67 per cent of its visible value is encouraging, since the orientation of this liquid crystal can be switched electronically both ways from parallel to orthogonal to the millimeter wave E-vector by simply changing the frequency of the applied voltage (for example, from 100 Hz to 10 kHz).

The birefringence did not vary greatly with the frequency of the microwave or millimeter wave being used in the 15–94 GHz range, as indicated in table 2 for BDH-E7 and ROTN-404. The estimated Δn values for E7 changed from 0·11 and 0·16 over the whole range; the preliminary network analyser studies gave lower values than the phase bridge studies. For example, at 30 GHz the network analyser Δn values for BDH-E7 and ROTN-404 were 0·11 and 0·14 compared to 0·16 and 0·17 from the phase bridge experiments. More complete studies will be required to evaluate the effects of different millimeter wave frequencies in more detail, but the results in table 2 indicate that the millimeter wave birefringence values are fairly flat over a wide range of frequencies.

The millimeter phase modulation obtained by reorientation of liquid crystals is reciprocal in regard to the propagation direction of millimeter wave. For example, a 30 GHz slot linear array antenna 18 cm long has been made, filled with liquid crystal, and used with external H-field alignment to demonstrate the capability of the linear angle scanning of both emitting and receiving radar signals by liquid crystal reorientation [8].

3.2. *E-Field versus H-field orientation of liquid crystals*

Millimeter wave phase modulation studies were also made in which electrical fields were used to reorient liquid crystals previously aligned by magnetic fields and vice versa. Typical results are shown in figure 7, in which the phase change was measured for two liquid crystals at several path lengths when the orientation was changed from E-field alignment parallel to the millimeter wave E-vector to H-field alignment perpendicular to the E-vector. At the field strengths indicated in figure 7, the millimeter wave Δn values for ROTN-404 and BDH-E7 were in good agreement with those shown in table 1. The response times for E-field orientation of BDH-E7 are shown in figure 8 as a function of the applied voltage across the waveguide cell (0·35 cm between electrodes), starting with random alignment. The response times at low voltages are very slow, but decreased to 1·5 s at about 300 V and then levelled off. In this experiment, the response time was proportional to $V^{-1\cdot65}$ over most of the applied voltage range, which is different from the common V^{-2} proportionality. This behaviour and the levelling off in the response times above 300 V is attributed to back flow effects in the bulk liquid crystal [9], and also to the slow response time of the phase shifter read out equipment. The waveguide cell surfaces have virtually no effect on the liquid crystal bulk in these cells with 3·5 mm between the electrodes, and there is virtually no threshold voltage for the start of field alignment. Correspondingly, the relaxation time for spontaneous randomization of liquid crystal orientation after removal of the E-field can be many hours, depending upon the extent of convection currents effects.

A 30 GHz liquid crystal electronic waveguide phase shifter had been made in a design combining both fixed magnets and electrodes [10]. In this device, the strength of the orthogonal magnetic field established a threshold voltage for the E-field reorientation and also reoriented the liquid crystal when the voltage was turned off.

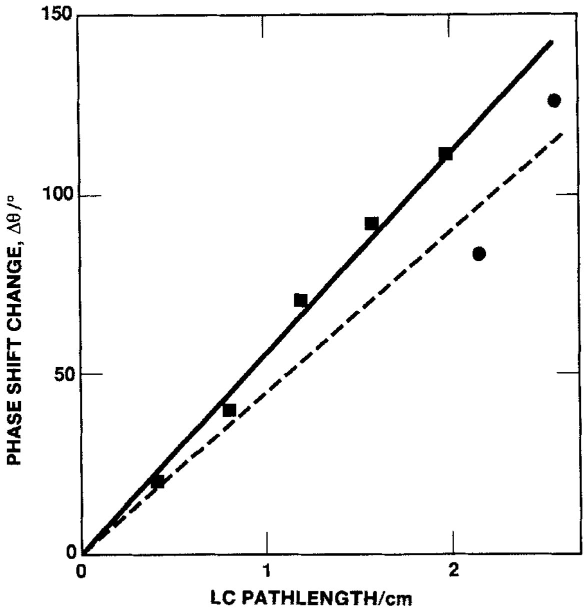

Figure 7. Path length effects on the phase shift from two liquid crystals (ROTN-404 (■) and BDH-E7 (●)) whose orientation was switched between orthogonal electric (300 V/0·35 cm) and magnetic fields (3 kG), parallel and perpendicular respectively to the E-vector of 30 GHz millimeter wave.

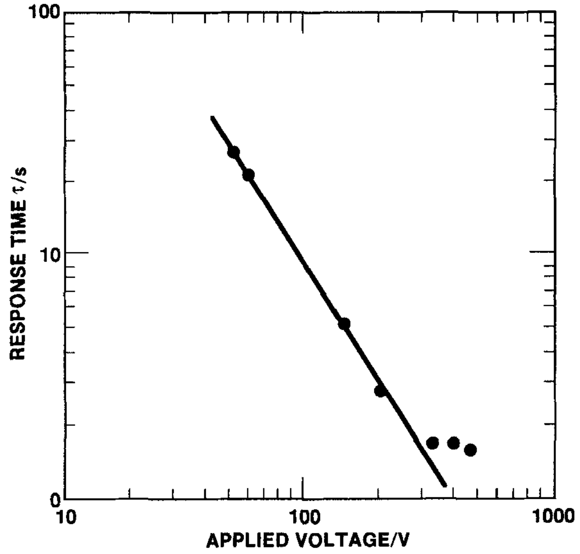

Figure 8. Response time of liquid crystal (BDH-E7) orientation in a waveguide cell as a function of applied voltages applied to electrodes separated by 0·35 cm; $\tau \propto V^{-1\cdot65}$.

3.3. *E-Field versus surface orientation*

We have studied several methods to obtain surface alignment forces on the liquid crystals used in millimeter wave devices. One method was to use the liquid crystal as small droplets contained in a solid matrix, such as in a polymer dispersed liquid crystal. A solid block of polymer dispersed liquid crystal was made by ultraviolet polymerization of a solution of 55 per cent BDH-E7 in Norland-NOA65 optical cement. This polymer dispersed liquid crystal block was 2·2 cm long and had a cross section size to fit into a 30 GHz waveguide. Electrodes were attached directly to two sides of the polymer dispersed liquid crystal block and it was slipped into a waveguide cell of the type shown in figure 4, except that the waveguide wall was cut away in the area of the electrodes. The phase shifts obtained with applied voltages across this polymer dispersed liquid crystal are shown in figure 9. There is a threshold voltage of about 100 V to obtain the initial phase shift. The response time at full on voltage (700 V, corresponding to 2·2 kV/cm) was 1 s and the spontaneous decay time upon removal of the field was also 1 s. Thus, the polymer surfaces surrounding the liquid crystal droplets in this polymer dispersed liquid crystal established surface forces effective for off-state alignment of the liquid crystal droplets in the waveguide cell. However, the advantages of the relatively fast spontaneous realignment in the off-state were offset by the small values of the phase shifts obtained. There are a number of reasons for this limited phase shift, including the following: (*a*) typically in this type of polymer dispersed liquid crystal less than 40 per cent of the total volume is in the form of liquid crystal droplets [11]; (*b*) because the applied field strength (2·2 kV/cm) was small for such polymer dispersed liquid crystals, only the larger droplets could be oriented by the E-field, while many other droplets were too small to be affected; (*c*) in this polymer dispersed liquid crystal the droplets were not pre-aligned, so that the droplets large enough to be aligned by the E-field were randomly aligned in the off-state, giving a smaller phase shift than had the droplets been pre-aligned orthogonal to the E-field direction.

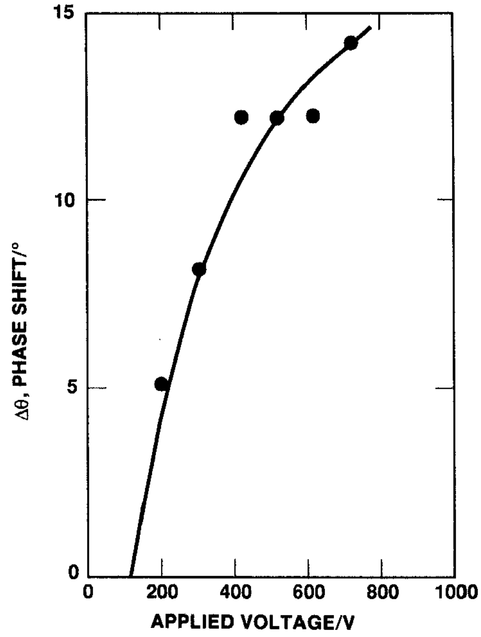

Figure 9. Effect of applied voltage on the phase shift of a block of polymer dispersed liquid crystal in a 30 GHz waveguide cell, using electrodes on two opposite sides of a polymer dispersed liquid crystal block 0·32 cm wide and 2·2 cm long. (The polymer dispersed liquid crystal block was prepared by ultraviolet exposure of 55 per cent BDH-E7 in Norland NOA-65.)

4. Conclusions

We have discovered and measured substantial birefringence values for a variety of thermotropic liquid crystals in the microwave millimeter wave region. This includes nematics with positive, negative, and crossover dielectric anisotropy, as well as a cholesteric liquid crystal. Preliminary correlations have been made on the liquid crystal structures which are favourable for high millimeter wave Δn values. Such structures appear to be those with highly conjugated, rod-like molecules in components containing tolane, terphenyl, and biphenylpyrimidine structures. However, this is a brand new field with many correlations yet to be made between liquid crystal structures and millimeter wave birefringence as well as millimeter wave loss effects.

We have described millimeter wave phase shifts in liquid crystal and polymer dispersed liquid crystal laboratory devices modulated by either (or both) magnetic and electric fields. These results have provided a basis for various types of modulators and scanning array antennae, especially in the millimeter wave (30–400 GHz) region where more compact liquid crystal modulation media can be used than in the lower frequency microwave region. These scanners can be used for simultaneous sending and receiving of radar signals. Such liquid crystal devices could greatly reduce the cost of phased array radar systems, and would be especially useful for applications where the required scan rates are relatively slow, such as about 0·1 to 10 scans per second.

References

[1] Wu, S.-T., 1991, *J. appl. Phys.*, **69**, 2080.
[2] Wu, S.-T., and Wu, C.-S., 1989, *J. appl. Phys.*, **66**, 5297.

[3] Wu, S.-T., 1987, *Opt. Engng*, **26,** 1722.
[4] Wu, S.-T., Efron, U., and Hess, L. D., 1984, *Appl. Phys. Lett.*, **44,** 1033.
[5] Stimson, G. W., 1983, *Introduction to Airborne Radar* (Hughes Aircraft Co.), p. 122.
[6] Debye, P., 1929, *Polar Molecules* (Chemical Catalog Co.), Chap. V.
[7] Afsar, M. N., and Button, K. J., 1984, *Infrared and Millimeter Waves*, Vol. 12, edited by K. J. Button (Academic Press), p. 12.
[8] Lim, K. C., 1990 (unpublished data).
[9] Blinov, L. M., 1988, *Electro-optical and Magneto-optical Properties of Liquid Crystals* (Wiley), p. 118.
[10] Lim, K. C., Margerum, J. D., and Lackner, A. M., 1992, *Appl. Phys. Lett* (in the press).
[11] Vaz, N. A., Smith, G. W., and Montgomery, G. P., Jr., 1987, *Molec. Crystals liq. Crystals*, **146,** 1.